GOSPODARKA SUROWCAMI MINERALNYMI – MINERAL RESOURCES MANAGEMENT

2025 Volume 41 Issue 2 Pages 161–175

DOI: 10.24425/gsm.2025.154548

DAWID MROCHEŃ[1], ANTON SROKA[2]

# Identification of Knothe's subsidence model parameters based on final subsidence values of individual pairs of points

## Introduction

Mining activities induce changes in the stress state of the rock mass, disrupting its existing equilibrium. The rock mass's tendency to reach a new equilibrium results in displacements within the rock structure toward the excavated void. This phenomenon can be described using a functional model that links the cause – constriction or convergence of the excavated space within the rock mass – with the effect – of surface displacements. Surface deformations often pose risks to structures and buildings located in developed areas affected by underground mining operations (Cempiel et al. 2023; Szojda and Kapusta 2023).

✉ Corresponding Author: Dawid Mrocheń; e-mail: dawid.mrochen@imgpan.pl

[1] Strata Mechanics Research Institute Polish Academy of Sciences, Kraków, Poland; AGH University of Krakow, Poland; ORCID iD: 0000-0003-0691-7947; Scopus ID: 57204184409; Researcher ID: ABD-2643-2022; e-mail: dawid.mrochen@imgpan.pl

[2] Strata Mechanics Research Institute Polish Academy of Sciences, Kraków, Poland; ORCID iD: 0000-0002-3932-4673; e-mail: sroka@imgpan.pl

Over the decades, starting from the first half of the 20th century, numerous geometrical-integral methods have been developed to predict the impact of underground mining operations on the Earth's surface (among others: Keinhorst 1925; Bals 1932; Beyer 1945; Sann 1949; Kochmański 1949, 1959; Knothe 1953; Litwiniszyn 1953). Nowadays, methods based on geometrical-integral models are still being developed and improved (Nicieza et al. 2005; Ren et al. 2014; Babaryka and Benndorf 2023). A comprehensive description of these methods can be found in numerous book publications, including but not limited to: (Kratzsch 1983; Peng 1992; Reddish and Whittaker 2012; Jiang et al. 2023). Regardless of whether the method is numerical or analytical, each must be adapted to local mining and geological conditions by defining boundary conditions and determining the optimal parameter values for the selected model. Selecting appropriate parameter values is crucial for the accuracy of displacement and deformation indices. For this reason, geometrical-integral models with a small number of parameters, which possess clear physical interpretation and significance, are particularly valued. The parameters of a geometrical-integral model can be determined by solving an inverse problem based on the observed displacement field (from geodetic measurements), to which the theoretical model converges through iterative computational methods (Dudek et al. 2024). In the absence of observational data, the computational model must adopt parameters characteristic of the specific mining region based on experience or relevant literature. The impact of using region-specific or mine-specific parameter values for predictions, as opposed to parameters determined from current geodetic measurements, was demonstrated by Gruszczyński (Gruszczyński et al. 2018). Using root mean square error (RMSE) on the observation line as a measure of prediction accuracy, Gruszczyński obtained an RMSE ranging from 436 mm when using average parameters for the mining region to 35 mm when employing current geodetic measurements. These results indicate that the appropriate selection of model parameters is crucial and significantly enhances the accuracy of predictive calculations.

Methods for determining the parameters of rock mass deformation models rely on levelling measurements. In the classical approach, geodetic observations are conducted using dedicated observational networks established for this purpose. Points stabilized above mining fields form observation lines, along which subsidence is measured. The height referencing of these observational networks must satisfy the condition of stability for the reference points over time. This implies that the reference points should be located outside the influence of mining operations. Consequently, in some cases, leveling reference lines may extend several kilometers, which can reduce the accuracy of height and subsidence determination for points in the observational network. Increasingly, satellite-based techniques are employed for height referencing, which helps mitigate errors in determining the heights of observational network points. The information obtained on subsidence along observation lines is used to determine the parameters of surface deformation models. This is typically achieved through least squares estimation procedures to match the profile of the observed subsidence trough to the theoretical one (Schober et al. 1987; Ścigała 2008; Kwinta 2011; Witkowski 2014; Gruszczyński et al. 2018). It is an iterative procedure that, in addition to the deformation model of the rock mass, requires the definition of initial parameter values, an objective function, and a convergence criterion. Depending on the approach, the search for the minimum of the objective function can be performed using various methods, such as the quasi-Newton method or the Hooke-Jeeves method. Nowadays, with the growing volume of observational data and the increasing number of parameters in deformation models, many researchers have explored the application of optimization and intelligent algorithms in the parameter inversion process (Chai et al. 2023).

In recent years, there has been significant development in remote sensing techniques used for measuring ground surface displacements (Blachowski et al. 2024). The advancement of satellite radar interferometry methods, such as Differential Interferometric Synthetic Aperture Radar (DInSAR) and Small Baseline Subset InSAR (SBAS InSAR), as well as LiDAR technology and the widespread adoption of Unmanned Aerial Vehicles (UAVs), has led to numerous efforts to utilize large-scale data acquired through these methods for determining surface deformation model parameters (Lei et al. 2024; Liu et al. 2024; Zhao et al. 2024). The integration of classical leveling measurements with satellite methods (GNSS) and satellite interferometry for monitoring mining areas also enables the identification of deformation model parameters for both the rock mass and the ground surface. Numerous studies in this field employ the Probability Integration Method (PIM) (Baochen and Guohua 1965). Li (Li et al. 2017, 2021) has adopted Genetic Algorithm (GA), which are probabilistic optimization techniques that can autonomously determine and guide the optimized search space, to determine the optimal parameters of the PIM model. Liu et al. (2022) utilized leveling measurement results, the SBAS InSAR method, and Geographically Weighted Regression. Based on Line of Sight (LOS) displacement values obtained via the InSAR method, Wang (Wang et al. 2018) determined the parameters of the PIM model, which was subsequently used to locate underground coal mining operations, including the depth and dimensions of mining panels.

Most methods for parameterizing deformation models are based on ground surface subsidence measurements. For horizontal displacement observations, geometric-integral methods (e.g., Knothe 1953, 1984; Baochen and Guohua 1965) require the determination of an additional parameter for horizontal displacements, which defines the magnitude of horizontal strain. This parameter can be estimated using satellite measurements (Tajduś et al. 2018), UAV measurements (Puniach et al. 2023), or theoretical calculations (Sroka et al. 2018a). Traditional measurement methods require significant labor related to the stabilization of observation points as well as the geodetic measurements themselves. The placement of monitoring networks for assessing mining impacts on the ground surface is often influenced by the existing transportation infrastructure, which may not always align with the optimal positioning relative to the mining field for determining model parameters. Data collected through such methods are discrete and confined to selected profiles above the mining activity, making inferences about the entire displacement field reliant on a limited portion of the subsidence trough.

Considering the limitations of conventional measurement methods, this article proposes a novel approach to parameterizing ground deformation models based on differential subsidence within the subsidence trough. Computational simulations demonstrate the high effectiveness of the proposed method, which significantly reduces the labor and associated costs of field measurements. Additionally, the approach does not require height reference points, enabling the calculation of subsidence differences across the entire displacement field. In many cases, the monitoring of mining impact areas involves a few isolated structures, such as public buildings (schools, hospitals, cultural facilities), sections of sewer pipelines, parts of rail transit routes, or the tilting of tall structures and chimneys. The focus of observation often lies in changes to slope or inclination, which are determined through relative subsidence difference measurements using leveling or electronic inclinometers. In such cases, the inclination of a single structural element measured with an electronic level can indirectly represent the subsidence difference over a segment with a length not exceeding a predefined distance, e.g., $0.1 \cdot r$ (where $r$ is the radius of the main influence range), oriented in the direction of the measurement.

## 1. Materials and methods

The article introduces an innovative method for determining the parameters of surface deformation models based on subsidence differences between pairs of points. This method relies on observations of asymptotic effects, i.e., the final state of the subsidence trough. The proposed approach is a universal solution applicable to computational models that utilize elevation observations for parameterization. Analyses and calculations were conducted using the widely applied geometric-integral Knothe model (Knothe 1953, 1957). Due to its effectiveness and versatility, the Knothe model has gained widespread recognition and is extensively used in the mining industry across Europe (Jiránková et al. 2020; Misa 2023), Asia (Lian et al. 2011), Australia (Byrnes 2003), and North America (Karmis et al. 2008). The basic version of the Knothe model has undergone numerous modifications, enabling it to simulate not only the effects of hard coal mining but also those of underground copper ore extraction (Hejmanowski 2004; Niedojadło et al. 2023), oil and natural gas production (Sroka and Hejmanowski 2006), rock salt mining (Hejmanowski and Malinowska 2017), the use of salt caverns for storing liquid and gaseous energy carriers (Schober et al. 1987; Tajduś et al. 2021), ground uplift due to the flooding of abandoned mines (Sroka 2005; Tajduś et al. 2023), subsidence caused by deep geothermal energy extraction (Sroka et al. 2018b) or surface deformation due to rock mass dewatering (Guzy and Witkowski 2021).

For mining operations of any shape and in cases where the exploited seam lies horizontally, the subsidence $s$ at any point on the ground surface can be expressed using a double integral over the boundaries of the mining area, as described by Knothe (Knothe 1953, 1957). This can be Equation (1):

$$s(x,y) = \frac{s_{\max}}{r^2} \iint_R \exp\left(-\pi \cdot \frac{(x-s)^2 + (y-t)^2}{r^2}\right) dsdt \tag{1}$$

↳ $s_{\max}$ – maximum subsidence, as given by Equation (2):

$$s_{\max} = a \cdot g \tag{2}$$

↳ $a$ – subsidence coefficient,
$g$ – thickness of mined seam,
$R$ – mined-out area,
$x, y$ – coordinates of the point where subsidence is calculated,
$r$ – radius of the main influence range, determined by Equation (3):

$$r = \frac{H}{\tan\beta} \tag{3}$$

↳ $H$ – depth of mining for a horizontally lying seam,
$\beta$ – angle of the main influence range, as defined by Knothe (Knothe 1953).

The estimation of the optimal values for the model parameters, i.e., $a$ and $\tan\beta$ based on observed subsidence differences for pairs of measurement points, allows for the reconstruction of the entire displacement field. The methodology for determining the parameter values is implemented as an inverse problem, based on the Gauss-Markov algorithm, in accordance with the criterion of minimizing the sum of squared deviations $V$ between the measurement results and the calculation results based on the identified values of the functional model parameters, as given by Equation (4):

$$V^T P V = \min! \tag{4}$$

↳ $P$ – weight matrix.

The content of the weight matrix may depend not only on the accuracy of individual subsidence difference measurements but also on the purpose of the analyses being conducted.

The Gauss-Markov algorithm is based on two models: the functional model of the analyzed phenomenon and the stochastic model of the performed observations. The functional model, represented by the Knothe solution, describes the causal relationship between mining activities and surface subsidence. The stochastic model expressed as a weight matrix $P$, accounts for the accuracy of the observations in the process of identifying the parameters of the functional model. For observations with equal accuracy, the matrix $P$ becomes an identity matrix. The approach relies on an iterative method for solving a system of linear equations that links mining activity to the observed effect in the form of subsidence differences between two points. The linearization of the Knothe formula (Knothe 1957) is performed using a Taylor series expansion while neglecting higher-order derivatives Equation (5):

$$\Delta s_i + v_i = \Delta s_i^0 + \left[\left(\frac{\partial s_j^i}{\partial a}\right)_0 - \left(\frac{\partial s_k^i}{\partial a}\right)_0\right]\cdot \hat{x}_1 + \left[\left(\frac{\partial s_j^i}{\partial \tan\beta}\right)_0 - \left(\frac{\partial s_k^i}{\partial \tan\beta}\right)_0\right]\cdot \hat{x}_2 \tag{5}$$

$\Delta s_i$ – the subsidence difference Equation (6) observed between the $i$-th pair of points:

$$\Delta s_i = s_j - s_k \tag{6}$$

$v_i$ – the correction to the observed subsidence difference,

$\Delta s_i^0$ – the computed value of the subsidence difference between the $i$-th pair of points for the initial parameter values $X_0(a_0, \tan\beta_0)$

$\left(\frac{\partial s_j^i}{\partial a}\right)_0$, $\left(\frac{\partial s_k^i}{\partial a}\right)_0$, $\left(\frac{\partial s_j^i}{\partial \tan\beta}\right)_0$, $\left(\frac{\partial s_k^i}{\partial \tan\beta}\right)_0$ – the partial derivatives for simulated subsidence values,

$s_j^i, s_k^i$ – the subsidence values of the observation points $j$ and $k$ forming the $i$-th difference,

$\hat{x}_1, \hat{x}_2$ – the unknowns to be determined.

The optimal values of the parameters $\hat{X}$ Equation (7) are determined using an iterative computation method, which enables successive approximations of the parameter values $X_0$ to be refined by the correction term $\hat{x}$ Equation (9) until convergence is achieved. The weight matrix $P$, which defines the accuracy of determining height differences in the case of equally precise observations, can be omitted:

$$\hat{X} = X_0 + \hat{x} \tag{7}$$

$$V = A\hat{x} - L \tag{8}$$

$$\hat{x} = \left(A^T PA\right)^{-1} \cdot A^T PL \tag{9}$$

A – the observation matrix Equation (10), for $n$-pairs of points, is constructed based on Equation (5):

$$A = \begin{bmatrix} \left(\frac{\partial s_j^1}{\partial a}\right)_0 - \left(\frac{\partial s_k^1}{\partial a}\right)_0 & \left(\frac{\partial s_j^1}{\partial \tan\beta}\right)_0 - \left(\frac{\partial s_k^1}{\partial \tan\beta}\right)_0 \\ \vdots & \vdots \\ \left(\frac{\partial s_j^n}{\partial a}\right)_0 - \left(\frac{\partial s_k^n}{\partial a}\right)_0 & \left(\frac{\partial s_j^n}{\partial \tan\beta}\right)_0 - \left(\frac{\partial s_k^n}{\partial \tan\beta}\right)_0 \end{bmatrix} \tag{10}$$

↳ $L$ – the matrix of free terms Equation (11), for $n$-pairs of points:

$$L = \begin{bmatrix} \Delta s_1 - \Delta s_1^0 \\ \vdots \\ \Delta s_n - \Delta s_n^0 \end{bmatrix} \tag{11}$$

The accuracy of the determined parameter values is measured by the root mean square error (RMSE) Equation (12):

$$RMSE = \sqrt{\frac{V^T V}{n-u}} \tag{12}$$

↳ $n$ – the number of observed pairs of elevation differences,
$u$ – the number of unknowns, $u = 2$,
$V$ – the vector of corrections Equation (8).

The standard deviations of the model parameters $s_a$ and $s_{\tan\beta}$ are determined based on the variance-covariance matrix $Q$ and the RMSE error Equations (12–15):

$$s_a = RMSE \cdot \sqrt{Q_{11}} \tag{13}$$

$$s_{\tan\beta} = RMSE \cdot \sqrt{Q_{22}} \tag{14}$$

$$Q = \left(A^T A\right)^{-1} \tag{15}$$

## 2. Results

As reference data for the presented method, simulated data were utilized to describe the asymptotic impacts of the completed mining activity. Calculations were performed for exploitation of a rectangular longwall panel with dimensions of 300 × 900 m (length × width) located horizontally at a depth of $H$ = 600 m. The mining thickness was $g$ = 3 m. For the simulation, the following Knothe model parameters were assumed as true values:

- $a = 0.85$,
- $\tan\beta = 2.15$.

For the parameters and boundary conditions defined as above, subsidence differences $\Delta s_i$ were calculated for 7 pairs of observation points distributed on the surface within the influence zone of the analyzed mining activity. The arrangement of the point pairs is random, with distances between the points ranging from $0.05 \cdot r$ to $0.15 \cdot r$, corresponding to distances in the range of 13.95–41.86 m (for $r$ = 279.08 m). The distances selected for the analysis represent the typical dimensions of buildings and structures, as well as the spacing of observation points along survey lines in mining areas in Poland. The mining scenario, including the locations of the observation point pairs, is illustrated in Figure 1, and the coordinates of the analyzed pairs are provided in Table 1.

The identification of the parameter values $a$ and $\tan\beta$ was performed using an iterative computation method, with the average values of the Knothe model parameters, characteristic of coal mining with roof collapse conditions in the Upper Silesian Coal Basin, Poland, assumed as initial parameters (Kowalski 2007; Gruszczyński et al. 2018):

- $a_0 = 0.80$,
- $\tan\beta_0 = 1.92$.

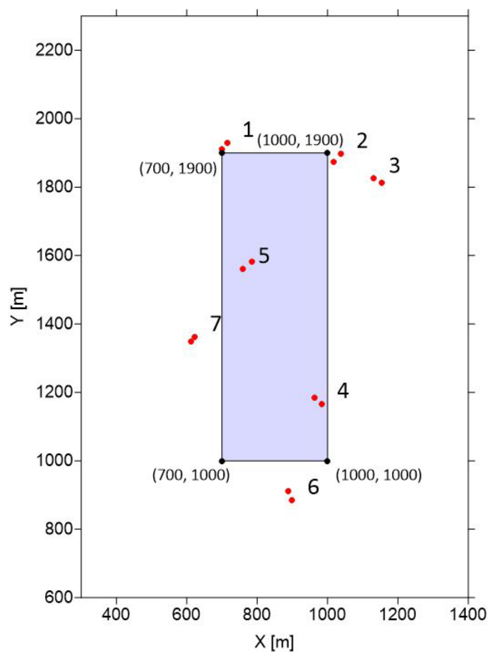


Fig. 1. The distribution of the observation point pairs against the background of the longwall panel

Rys. 1. Rozkład par punktów obserwacyjnych na tle pola ścianowego

Table 1. Characteristics of computational points

Tabela 1. Charakterystyka punktów obliczeniowych

| Pair no. | $X$ (m) | $Y$ (m) | Distance (m) | $\Delta s_i$ (mm) |
|---|---|---|---|---|
| 1 | 714 | 1,930 | 22.2 | 35.50 |
| | 701 | 1,912 | | |
| 2 | 1,038 | 1,898 | 32.6 | 193.15 |
| | 1,016 | 1,874 | | |
| 3 | 1,130 | 1,825 | 25.5 | –63.72 |
| | 1,153 | 1,814 | | |
| 4 | 984 | 1,167 | 27.7 | 194.32 |
| | 963 | 1,185 | | |
| 5 | 759 | 1,561 | 32.6 | 155.60 |
| | 784 | 1,582 | | |
| 6 | 899 | 886 | 28.6 | 132.48 |
| | 887 | 912 | | |
| 7 | 622 | 1,362 | 17.0 | –75.70 |
| | 611 | 1,349 | | |

For the iterative calculations, a stopping criterion was defined, i.e., the termination of the computations based on the condition that the increments of the unknowns between successive iterations meet a predefined threshold (16):

$$\Delta a < 0.01 \text{ and } \Delta \tan\beta < 0.05 \tag{16}$$

The obtained results (Table 2) indicate the high effectiveness of the presented method. It allows for the unambiguous identification of the model parameters based on relative measurements, i.e., the elevation differences. The optimal parameter values were determined according to the adopted criterion (16) in a single iteration, achieving values that are convergent with the true values.

Based on the determined parameter values, the surface subsidence basin was reconstructed (Figure 2). The maximum subsidence values obtained are located in the central part of the subsidence basin above the mining area, amounting to $s_{max}$ = –2.09 m. Utilizing the displacement field derived from measurements of individual building structures or buildings, it is possible to infer the impact of mining activities on other structures and infrastructure elements not covered by monitoring within the influence range of the conducted mining operations.

Table 2. Results of the iterative calculations

Tabela 2. Wyniki obliczeń iteracyjnych

| | Real values | Initial values | Iteration no. | |
|---|---|---|---|---|
| | | | 0 | 1 |
| $a$ | **0.85** | 0.80 | 0.8419 | **0.8500** |
| $\Delta a$ | | | 0.0419 | 0.0081 |
| $s_a$ | | | 0.0007 | 0.0000 |
| $\tan\beta$ | **2.15** | 1.92 | 2.1620 | **2.1499** |
| $\Delta\tan\beta$ | | | 0.2420 | 0.0121 |
| $s_{\tan\beta}$ | | | 0.0013 | 0.0000 |
| RMSE (mm) | | | 0.0725 | 0.0000 |

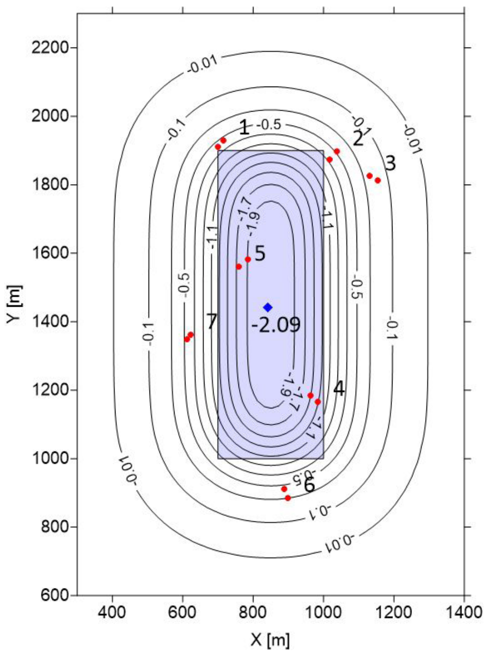


Fig. 2. The subsidence trough with the maximum subsidence (blue point) reconstructed based on the determined optimal model parameters

Rys. 2. Niecka osiadania z maksymalnym osiadaniem (punkt niebieski) zrekonstruowana na podstawie wyznaczonych optymalnych parametrów modelu

## 3. Discussion

The presented concept of using subsidence differences for individual structures within the displacement field allows for efficient and rapid identification of the computational model parameters. For accurate reconstruction of the subsidence basin, it is essential that the analyzed point pairs are located both in the central region and other areas of the subsidence basin.

Observed buildings and infrastructure elements are typically distributed over a relatively large area, meaning the observed subsidence differences represent various regions of the basin. Consequently, the parameters determined in this manner are based on the spatial distribution of surface deformation, in contrast to classical methods relying on observations conducted along observation lines forming terrain profiles. This approach can also be applied to data derived from satellite radar interferometry or UAV. The large volume of data from such monitoring can be reduced to a few or a dozen point pairs for which subsidence differences are calculated.

The Gauss-Markov algorithm, like many other optimization algorithms, is sensitive to initial parameter values. However, mining practices allow for the estimation of initial parameters based on prior experience (e.g., average values for the mining region or mine) or simple mathematical relationships (Wang et al. 2021). In the presented computational example, the optimal parameter values determined are identical to the true values, as the theoretical example assumes no errors related to the computational model's inadequacy in representing the actual geological structure. Additionally, the simulated subsidence differences (real values) are not affected by measurement errors.

## Conclusions

The presented article demonstrates that the innovative method for identifying the parameters of the geometric-integral Knothe method, based on measurements of subsidence differences from monitoring individual building and engineering structures in areas affected by mining activities, is fully effective. This method can be utilized to reconstruct the entire displacement field, assess the risks to unmonitored structures, and evaluate the anticipated future impacts of planned mining operations in the region on the land surface.

*The Authors have no conflict of interest to declare.*

## REFERENCES


Babaryka, A. and Benndorf, J. 2023. Ground Subsidence above Salt Caverns for Energy Storage: A Comparison of Prediction Methods with Emphasis on Convergence and Asymmetry. *Mining* 3(2), pp. 334–346, DOI: 10.3390/mining3020020.

Bals, R. 1932. Contribution to the question of forecasting mining subsidence (*Beitrag zur Frage der Vorausberechnung bergbaulicher Senkungen*). *Mitteilungen aus dem Markscheidewesen* 42/43, pp. 98–111 (*in German*).

Baochen, L. and Guohua, L. 1965. *Coal Mining Ground Surface Movements*. Chinese Industry Press, Beijing.

Beyer, F. 1945. *Über die Vorausbestimmung der beim Abbau flachgelagerter Flötze aufreten den Bodenverformungen* (Habilitationsschrift). TU Berlin.

Blachowski et al. 2024 – Blachowski, J., Wajs, J., Walerysiak, N. and Becker, M. 2024. Monitoring of post--mining subsidence using airborne and terrestrial laser scanning approach. *Archives of Mining Sciences* 69, pp. 431–446, DOI: 10.24425/ams.2024.151444.

Byrnes, R. 2003. Case Studies in the Application of Influence Functions to Visualising Surface Subsidence. *Conference. University of Wollongong & the Australasian Institute of Mining and Metallurgy*, pp. 90–100.

Cempiel et al. 2023 – Cempiel, E., Strzalkowski, P., Ścigala, R., Bryt-Nitarska, I. 2023. Assessment of damage causes of monumental objects located in mining areas – case study. *Archives of Mining Sciences* 68, pp. 187–205, DOI: 10.24425/ams.2023.146175.

Chai et al. 2023 – Chai, H., Xu, M., Guan, P., Ding, Y., Xu, H. and Zhao, Y. 2023. Research on Mining Subsidence Prediction Parameter Inversion Based on Improved Modular Vector Method. *Applied Sciences* 13(24), DOI: 10.3390/app132413272.

Dudek et al. 2024 – Dudek, M., Mrocheń, D., Sroka, A. and Tajduś, K. 2024. Integrating the Finite Element Method with Python Scripting to Assess Mining Impacts on Surface Deformations. *Applied Sciences* 14(17), DOI: 10.3390/app14177797.

Gruszczyński et al. 2018 – Gruszczyński, W., Niedojadło, Z. and Mrocheń, D. 2018. Influence of model parameter uncertainties on forecasted subsidence. *Acta Geodynamica et Geomaterialia* 15(3), pp. 211–228, DOI: 10.13168/AGG.2018.0016.

Guzy, A. and Witkowski, W.T. 2021. Land Subsidence Estimation for Aquifer Drainage Induced by Underground Mining. *Energies* 14(15), DOI: 10.3390/en14154658.

Hejmanowski, R. 2004. *Modelling in time and space of deformation caused by open stope mining in a layered orebody*. Kraków: Uczelniane Wydawnictwa Naukowo-Dydaktyczne AGH (*in Polish*).

Hejmanowski, R. and Malinowska, A.A. 2017. Land subsidence inversion method application for salt mining-induced rock mass movement. *Gospodarka Surowcami Mineralnymi – Mineral Resources Management* 33(3), pp. 179–200, DOI: 10.1515/gospo-2017-0034.

Jiang et al. 2023 – Jiang, Y., Preusse, A., Sroka, A., Misa, R., Gao, J., Yang, Z., Jiang, Yue, Xu, Y., Zhang, X., Tajduś, K., Kateloe, H.J. and Frenz, W. 2023. *Theory and Application of Prediction of Surface Movement and Deformation Caused by Underground Mining*. China University of Mining and Technology Press.

Jiránková et al. 2020 – Jiránková, E., Waclawik, P. and Nemcik, J. 2020. Assessment of models to predict surface subsidence in the Czech part of the upper silesian coal basin-case study. *Acta Geodynamica et Geomaterialia* 17(4), pp. 469–484, DOI: 10.13168/AGG.2020.0034.

Karmis et al. 2008 – Karmis, M., Agioutantis, Z. and Andrews, K. 2008. Enhancing Mine Subsidence Prediction and Control Methodologies. *27$^{th}$ International Conference on Ground Control in Mining.* Morgantown, West Virginia, USA, 29–31 July, pp. 131–136.

Keinhorst, H. 1925. Die *Berechnung der Bodensenkungen im Emschergebiet. Festschrift 25 Jahre der Emschergenossenschaft 1900–1925.* Essen, Germany.

Knothe, S. 1953. A profile equation for a definitely shaped subsidence trough. *Archives of Mining Steel Industry* 1, pp. 22–38.

Knothe, S. 1957. Observations of surface movements under influence of mining and their theoretical interpretation. *Conference Proceedings European Congress on Ground Movement*. Leeds, pp. 210–218.

Knothe, S. 1984. *Prediction of mining influence* (*Prognozowanie wpływów eksploatacji górniczej*). Katowice: Śląsk Publishing House (*in Polish*).

Kochmański, T. 1949. Horizontal and vertical ground shifts due to mining reconstruction (*Przesunięcia terenu i w pionie i poziomie pod wpływem odbudowy górniczej*). *Hutnik* 7–8 (*in Polish*).

Kochmański, T. 1959. *Integral-Theorie der Bodenbewegungen unter Einwirkung des Abbaus*. Freiberger Forschungshefte A118, 36–58.

Kowalski, A. 2007. Undetermined Mining Surface Deformation in Terms of the Accuracy of Projections (*Nieustalone górnicze deformacje powierzchni w aspekcie dokładności prognoz*). *Studia – Rozprawy – Monografie* 871, Katowice: GIG (*in Polish*).

Kratzsch, H. 1983. *Mining Subsidence Engineering*. Springer-Verlag, Berlin Heidelberg New York.

Kwinta, A. 2011. Application of the least squares method in determination of the Knothe deformation prediction theory parameters. *Archive of Mining Sciences* 56(2), pp. 319–329.

Lei et al. 2024 – Lei, M., Zhang, T., Shi, J. and Yu, J. 2024. InSAR-CTPIM-Based 3D Deformation Prediction in Coal Mining Areas of the Baisha Reservoir, China. *Applied Sciences* 14(12), DOI: 10.3390/app14125199.

Lian et al. 2011 – Lian, X., Jarosz, A., Saavedra-Rosas, J. and Dai, H. 2011. Extending dynamic models of mining subsidence. *Transactions of Nonferrous Metals Society of China* 21, pp. s536–s542, DOI: 10.1016/S1003-6326(12)61637-9.

Li et al. 2017 – Li, P., Peng, D., Tan, Z. and Deng, K. 2017. Study of probability integration method parameter inversion by the genetic algorithm. *International Journal of Mining Science and Technology* 27, pp. 1073–1079, DOI: 10.1016/j.ijmst.2017.06.006.

Li et al. 2021 – Li, J., Yu, X., Liang, Y. and Chi, S. 2021. Parameter Solving of Probability Integral Method Based on Improved Genetic Algorithm. *Tehnicki vjesnik – Technical Gazette* 28(2), DOI: 10.17559/TV-20200429150210.

Litwiniszyn, J. 1953. Differential equation of rock displacement (*Równanie różniczkowe przemieszczeń górotworu*). *Archives of Mining Steel Industry* 1(1), pp. 9–21 (*in Polish*).

Liu et al. 2022 – Liu, H., Li, M., Yuan, M., Li, B. and Jiang, X. 2022. A fine subsidence information extraction model based on multi-source inversion by integrating InSAR and leveling data. *Natural Hazards* 114(3), pp. 2839–2854, DOI: 10.1007/s11069-022-05494-6.

Liu et al. 2024 – Liu, H., Yuan, M., Li, M., Li, B., Chen, N., Wang, J., Li, X. and Wu, X. 2024. TDFPI: A Three-Dimensional and Full Parameter Inversion Model and Its Application for Building Damage Assessment in Guotun Coal Mining Areas, Shandong, China. *Remote Sensing* 16(4), DOI: 10.3390/rs16040698.

Misa, R. 2023. Knothe's theory parameters – computational models and examples of practical applications. *Gospodarka Surowcami Mineralnymi – Mineral Resources Management* 39(4), 157–180, DOI: 10.24425/gsm.2023.148164.

Nicieza et al. 2005 – Nicieza, C.G., Álvarez Fernández, M.I., Menéndez Díaz, A. and Álvarez Vigil, A.E. 2005. The new three-dimensional subsidence influence function denoted by n–k–g. *International Journal of Rock Mechanics and Mining Sciences* 42(3), pp. 372–387, DOI: 10.1016/j.ijrmms.2004.12.003.

Niedojadło et al. 2023 – Niedojadło, Z., Stoch, T., Jura, J., Sopata, P., Wójcik, A. and Mrocheń, D. 2023. Monitoring and modelling the deformation state of a dyke of a flotation tailings reservoir of a copper ore mine. *Acta Montanistica Slovaca* 28(1), pp. 123–140, DOI: 10.46544/AMS.v28i1.11.

Peng, S.S. 1992. *Surface subsidence engineering*. Society for Mining, Metallurgy, and Exploration Littleton, CO (USA).

Puniach et al. 2023 – Puniach, E., Gruszczyński, W., Stoch, T., Mrocheń, D., Ćwiąkała, P., Sopata, P., Pastucha, E. and Matwij, W. 2023. Determination of the coefficient of proportionality between horizontal displacement and tilt change using UAV photogrammetry. *Engineering Geology* 312(1), DOI: 10.1016/j.enggeo.2022.106939.

Reddish, D.J. and Whittaker, B.N. 2012. *Subsidence: Occurrence, Prediction and Control*. Elsevier Science.

Ren et al. 2014 – Ren, G., Li, G. and Kulessa, M. 2014. Application of a Generalised Influence Function Method for Subsidence Prediction in Multi-seam Longwall Extraction. *Geotechnical and Geological Engineering* 32, pp. 1123–1131.

Sann, B. 1949. Considerations for the prediction of land subsidence due to coal mining (*Betrachtungen zur Vorausberechnung von Bodensenkungen infolge Kohen abbaus*). *Bergbau Rundschau* 1, pp. 163–168 (*in German*).

Schober et al. 1987 – Schober, F., Sroka, A. and Hartmann, A. 1987. A concept for predicting subsidence over cavern fields (*Ein Konzept zur Senkungsvorausberecnung über kavernfeldern*). *Kali und Steinsaltz* 9, pp. 374–379 (*in German*).

Ścigała, R. 2008. Computer-aided forecasting of rock mass and surface deformations caused by underground mining (*Komputerowe wspomaganie prognozowania deformacji górotworu i powierzchni wywołanych podziemną eksploatacją górniczą*). Gliwice: P.Śl. (*in Polish*).

Sroka, A. 2005. A contribution to the forecast of uplifts caused by the rise in mine water (*Ein Beitrag zur Vorausberechnung der durch den Grubenwasseranstieg bedingten Hebungen*). [In:] *Conference Proceedings 5. Altbergbaukolloquium, Technische Universität Clausthal.* Verlag Glückauf, Essen, pp. 453–464 (*in German*).

Sroka, A. and Hejmanowski, R. 2006. Subsidence prediction caused by the oil and gas development. [In:] *Proceedings of the 3rd/12th FIG Symposium.* Baden, Germany, 22–24 May 2006.

Sroka et al. 2018a – Sroka, A., Misa, R. and Tajduś, K. 2018a. Determination of the horizontal deformation factor for mineral and fluidized deposits exploitation. *Acta Geodynamica et Geomaterialia* 15, pp. 23–26, DOI: 10.13168/AGG.2017.0030.

Sroka et al. 2018b – Sroka, A., Misa, R. and Tajduś, K. 2018b. Modern applications of the Knothe theory in calculations of surface and rock mass deformations. *Prace Instytutu Mechaniki Górotworu PAN* 20, pp. 111–122.

Szojda, L. and Kapusta, L. 2023. Numerical analysis of buildings located on the edge of the post-mining basin. *Archives of Mining Sciences* 68(1), pp. 125–140, DOI: 10.24425/ams.2023.144321.

Tajduś et al. 2018 – Tajduś, K., Misa, R. and Sroka, A. 2018. Analysis of the surface horizontal displacement changes due to longwall panel advance. *International Journal of Rock Mechanics and Mining Sciences* 104, pp. 119–125, DOI: 10.1016/j.ijrmms.2018.02.005.

Tajduś et al. 2021 – Tajduś, K., Sroka, A., Misa, R., Tajduś, A. and Meyer, S. 2021. Surface deformations caused by the convergence of large underground gas storage facilities. *Energies* 14(2), DOI: 10.3390/en14020402.

Tajduś et al. 2023 – Tajduś, K., Sroka, A., Dudek, M., Misa, R., Hager, S. and Rusek, J. 2023. Effect of the Entire Coal Basin Flooding on the Land Surface Deformation. *Archives of Mining Sciences* 68(3), pp. 375–392, DOI: 10.24425/ams.2023.146857.

Wang et al. 2018 – Wang, L., Wei, T., Li, N., Chi, S., Jiang, C. and Fang, S. 2018. Research on probability integration parameter inversion of mining-induced surface subsidence based on quantum annealing. Environ Earth Sci 77(21), DOI: 10.1007/s12665-018-7927-z.

Witkowski, W.T. 2014. Implementation of the least squares method in determining the parameters of Knothe's theory. *Geomatics and Environmental Engineering* 8(3), DOI: 10.7494/geom.2014.8.3.107.

Zhao et al. 2024 – Zhao, J., Niu, Y., Zhou, Z., Lu, Z., Wang, Z., Zhang, Z., Li, Y. and Ju, Z. 2024. Construction of Mining Subsidence Basin and Inversion of Predicted Subsidence Parameters Based on UAV Photogrammetry Products Considering Horizontal Displacement. *Remote Sens* 16(22), DOI: 10.3390/rs16224283.

## IDENTIFICATION OF KNOTHE'S SUBSIDENCE MODEL PARAMETERS BASED ON FINAL SUBSIDENCE VALUES OF INDIVIDUAL PAIRS OF POINTS

Keywords

subsidence differences, Gauss-Markov algorithm, Knothe model, parameterization

Abstract

The article presents an innovative method for parameter identification of the Knothe integral--geometric model, which is based on analyzing subsidence differences for pairs of points. This method leverages observations from monitoring the displacements of buildings and engineering structures in areas affected by mining activities. By utilizing relative observations, i.e., differences in subsidence between point pairs for individual structures, elevation benchmarks are not needed during measurements. A key assumption of the methodology is the use of the asymptotic subsidence state, corresponding to the final stage of subsidence trough formation. Model parameters are iteratively determined by solving the inverse problem using the Gauss-Markov algorithm. This approach minimizes the sum of squared differences between the measured and calculated subsidence differences, enabling precise parameter fitting to the observed data. The implementation of a computation stop criterion concludes the iterative process of parameter identification. This criterion is based on achieving convergence in the form of a defined change in the estimated parameter values of the model between iterations, ensuring the efficiency and stability of the computations. The practical applicability of the method was validated using simulation data, confirming its capability to reconstruct the entire displacement field. The results enable not only the assessment of risk for unmonitored structures but also the prediction of future impacts of planned mining operations on the surface of the studied region.

## IDENTYFIKACJA PARAMETRÓW MODELU OSIADANIA KNOTHEGO W OPARCIU O KOŃCOWE WARTOŚCI OSIADANIA POJEDYNCZYCH PAR PUNKTÓW

S ł o w a k l u c z o w e

parametryzacja, różnice obniżeń, model Knothego, algorytm Gaussa-Markowa

S r e s z c z e n i e

W artykule zaprezentowano nowatorską metodę identyfikacji parametrów modelu całkowo-geometrycznego Knothego, która opiera się na analizie różnic osiadania dla par punktów. Metoda ta pozwala na wykorzystanie obserwacji pochodzących z monitorowania przemieszczeń budynków i konstrukcji inżynierskich na obszarach oddziaływania działalności górniczej. Dzięki wykorzystaniu obserwacji względnych, tj. różnic obniżeń par punktów dla pojedynczych obiektów budowlanych, nie jest wymagane nawiązanie wysokościowe dla wykonywanych pomiarów wysokościowych. Kluczowym założeniem metodologii było wykorzystanie asymptotycznego stanu osiadania, który odpowiada końcowemu etapowi formowania się niecki osiadania. Parametry modelu są iteracyjnie wyznaczane poprzez rozwiązywanie problemu odwrotnego za pomocą algorytmu Gaussa-Markowa. Metoda ta minimalizuje sumę kwadratów różnic między zmierzonymi a obliczonymi wartościami różnic osiadania, co pozwala na precyzyjne dopasowanie parametrów do obserwowanych danych. Zastosowanie kryterium stopu obliczeń kończy iteracyjny proces identyfikacji parametrów. Kryterium to polega na osiągnięciu zbieżności w postaci zdefiniowanego przyrostu wyznaczonych wartości parametrów modelu między iteracjami, co gwarantuje efektywność i stabilność obliczeń. Praktyczną użyteczność metody zweryfikowano przy użyciu danych symulacyjnych, co potwierdziło możliwość rekonstrukcji całego pola przemieszczeń. Otrzymane wyniki umożliwiają nie tylko ocenę ryzyka dla niemonitorowanych obiektów, ale także prognozowanie przyszłych oddziaływań planowanych operacji górniczych na powierzchnię terenu w badanym regionie.